frontiers | Frontiers in Coatings, Dyes and Interface Engineering

TYPE Original Research
PUBLISHED 21 February 2025
DOI 10.3389/frcdi.2025.1531144

OPEN ACCESS

EDITED BY
Salvio Suárez-García,
Catalan Institute of Nanoscience and Nanotechnology (CIN2), Spain

REVIEWED BY
Tuba Cakir Canak,
Istanbul Technical University, Türkiye
Juan Mancebo-Aracil,
CONICET Institute of Southern Chemistry (INQUISUR), Argentina

*CORRESPONDENCE
Radosław Mrówczyński,
radoslaw.mrowczynski@amu.edu.pl

RECEIVED 19 November 2024
ACCEPTED 24 January 2025
PUBLISHED 21 February 2025

CITATION
Ostrowska S, Szukowska M, Kim S, Kim Y, Wawrzyniak D and Mrówczyński R (2025) Doxorubicin and sorafenib release from mesoporous silica nanoparticles coated with polydopamine – influence of mechanical and chemical stimuli on the process.
Front. Coat. Dye In. 3:1531144.
doi: 10.3389/frcdi.2025.1531144

Doxorubicin and sorafenib release from mesoporous silica nanoparticles coated with polydopamine – influence of mechanical and chemical stimuli on the process

Sylwia Ostrowska[1,2], Monika Szukowska[1,2], Shinik Kim[3], Yeonho Kim[3], Dariusz Wawrzyniak[4] and Radosław Mrówczyński[1,2]*

[1]Faculty of Chemistry, Adam Mickiewicz University, Poznań, Poland, [2]Center for Advanced Technologies, Adam Mickiewicz University, Poznań, Poland, [3]Department of Applied Chemistry, Konkuk University, Chungju, Republic of Korea, [4]Department of Molecular Neurooncology, Institute of Bioorganic Chemistry, Polish Academy of Sciences, Poznań, Poland

In this paper, we present results of a study on the influence of different experimental conditions on drug release, for the two anticancer drugs: doxorubicin (DOX) and sorafenib (SO), from mesoporous silica nanoparticles coated with polydopamine (PDA) shell. We tested the drugs release from the carrier into buffers of different pH (4.5; 5.5; 7.5) and with the addition of H_2O_2 or glutathione (GSH), while stirring the carriers in a flask or shaking them in a thermoblock, keeping the same time intervals, temperature and frequency. The obtained results and performed statistical analysis prove that the way the drug release tests are conducted has a significant influence on the efficiency of release of both drugs from the carrier. Thus, our results are of great importance for characterization of multimodal nanocarriers for biomedical application in terms of drug release and bring new knowledge for their methodological investigation.

KEYWORDS

polydopamine, drug release, silica nanoparticles, sorafenib, doxorubicin

1 Introduction

The fight against neoplastic diseases is one of the most important challenges that modern science has to face since cancer is one of the main causes of mortality, resulting in approximately 18 million deaths annually (Zajda et al., 2021; Wang et al., 2021). Nowadays, cancer is mostly treated by conventional approaches like chemotherapy, surgical resection and radiotherapy. However, these methods are highly aggressive, non-specific, and often accompanied by significant side effects, because the agents they employ also show conspicuous toxicity to normal cells and tissues (Ceresa et al., 2014; Tao et al., 2015). Therefore, the use of nanoparticles as drug carriers of low toxicity, higher efficiency and stability than conventional dosage forms, allowing sustained and controlled anticancer drug delivery for altering signal transduction or modulating the tumour microenvironment, are

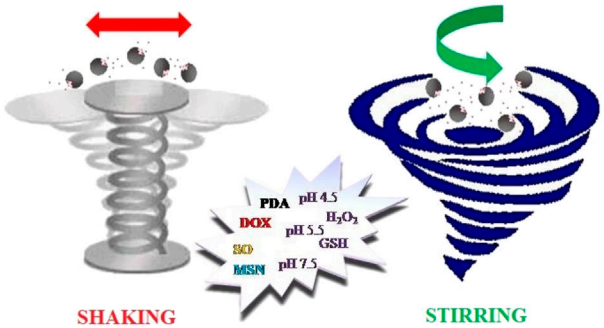

GRAPHICAL ABSTRACT

considered a game-changer in the field of novel cancer therapies (Barba et al., 2014; Chang et al., 2016). Moreover, the advantages of nanotechnology-based drug carriers include the small sizes compatible with intravenous injection and large surface area per unit volume amenable to modification for targeted delivery (Langer, 1998; Petros and Desimone, 2010; Shi et al., 2010; Li T et al., 2019). Furthermore, nanocarriers that can deliver drugs in a spatiotemporally controlled manner, enhance therapeutic efficacy of the drugs. That is why the nanocarriers reduce systemic side effects of cytostatic drugs, which results in improved patient's condition, allowing reduction of the dose and administration frequency. To develop nanocarriers with desirable release kinetics for targeted applications, it is important to understand the mechanisms of drug retention and release, the effects of the carrier composition, surface charge, hydrophilicity and morphology on the drug release kinetics, and techniques for nanocarriers preparation and modification. Temporal control over the drug release from the carriers is implemented to maintain drug concentration in blood or targeted tissues at the efficacious level. Since the first report of sustained drug release from polymeric carriers in 1964 (Folkman and Long, 1964), temporal control of drug release from different nanocarriers has been extensively studied, which permitted development of several mathematical models describing drug releases kinetics from drug delivery systems, such as the zero order model, first order model, Huguchi model, Hixson-Crowell model, Korsmeyer-Peppas model, and regression model (Dash et al., 2010; Paarakh et al., 2019; Singhvi and Singh, 2011).

In recent years, mesoporous silica nanoparticles (MSN) have attracted much attention due to simple synthesis, tunable pore size and volume, easy functionalization and excellent biocompatibility. Mesoporous silica nanoparticles contain a complex 'worm-like' network of channels throughout the interior, so they have large surface areas and extraordinarily high drug loading capacity (Wang et al., 2021; Gao et al., 2020; Kankala et al., 2022; Vallet-Regí et al., 2017; Li X et al., 2019). Moreover, these particles remain stable over broad ranges of temperature and pH, and can be used to deliver large doses of drugs or nucleic acids in a controlled manner (Wang et al., 2021; Kankala et al., 2022; Muhammad et al., 2014). However, to keep drug molecules inside the pores of MSNs and to control their release, some "gatekeepers" are required on the MSNs surface (Ashley et al., 2011; Muhammad et al., 2011).

Lately, PDA has been introduced as a material than can be used as a "gatekeeper" for MSN (Wei et al., 2017; Li et al., 2018). This material has drawn attention of different scientific groups as it shows sensitivity to pH, high biocompatibility and offers a possibility of further functionalization (Mrówczyński et al., 2015; Woźniak et al., 2017; Mrówczyński et al., 2016; Grześkowiak et al., 2021). The PDA coating can also endow MSNs and other nanostructures with photothermal properties (Mrówczyński, 2018). There are only a few papers that describe the use of the MSN-PDA system for the controlled release of drugs. In 2014, Zheng et al. reported that DOX can be released from such carriers in acidic media, while the drug remained inside the particles in the neutral media (Zheng et al., 2014). A novel pH-sensitive drug delivery system modified with PDA for controlled release of cationic amphiphilic drug desipramine (DES) was prepared by Zeng and co-workers. MSN@DES@PDA had high drug loading capacity and allowed a release of DES in a pH responsive manner. Importantly, the DES release profiles from the MSN@DES and MSN@DES@PDA were totally different. Moreover, the drug release from MSN@DES@PDA accelerated with increasing acidity (Chang et al., 2016). In another report, Yuan et al. presented MSNs coated with PDA conjugated with keratin via iron (III)-mediated coordination chemistry. The synthesized nanoparticles MSNs(MSN-DOX@PDA@keratin) exhibited pH and glutathione (GSH) dual-responsive drug release behavior as well as higher toxicity against tumor cells, while keeping low toxicity towards normal cells (Du et al., 2021). Recently, Wang's and Tan's research groups proposed a facile biphasic approach based on the use of hollowed GSH-sensitive tetrasulfide bonded mesoporous silica co-doped with PDA, in the silicone skeleton fabrication for synergistic therapy of breast cancer (Hu et al., 2022). The biocompatible and biodegradable PhMOSN had an ideal large surface area for DOX loading. After hyaluronic acid (HA) coating on the surface on the hollowed nanoparticle, PhMOSN@DOX-HA showed no drug leakage in normal tissue, while it gradually released the drug under high GSH level (Hu et al., 2022).

In this paper, we present the synthesis of a pH-sensitive drug delivery system based on mesoporous silica nanoparticles (MSNs) modified with polydopamine (PDA) designed for controlled release of hydrophilic DOX and hydrophobic drug sorafenib. MSN@drug@PDA carries were subjected to physical investigation to determine their size, surface morphology, pore size as well as their zeta potential and structure. We also carried out profound studies on the drug loading and drug release behavior, dependent on the experimental conditions used for this process, like shaking or

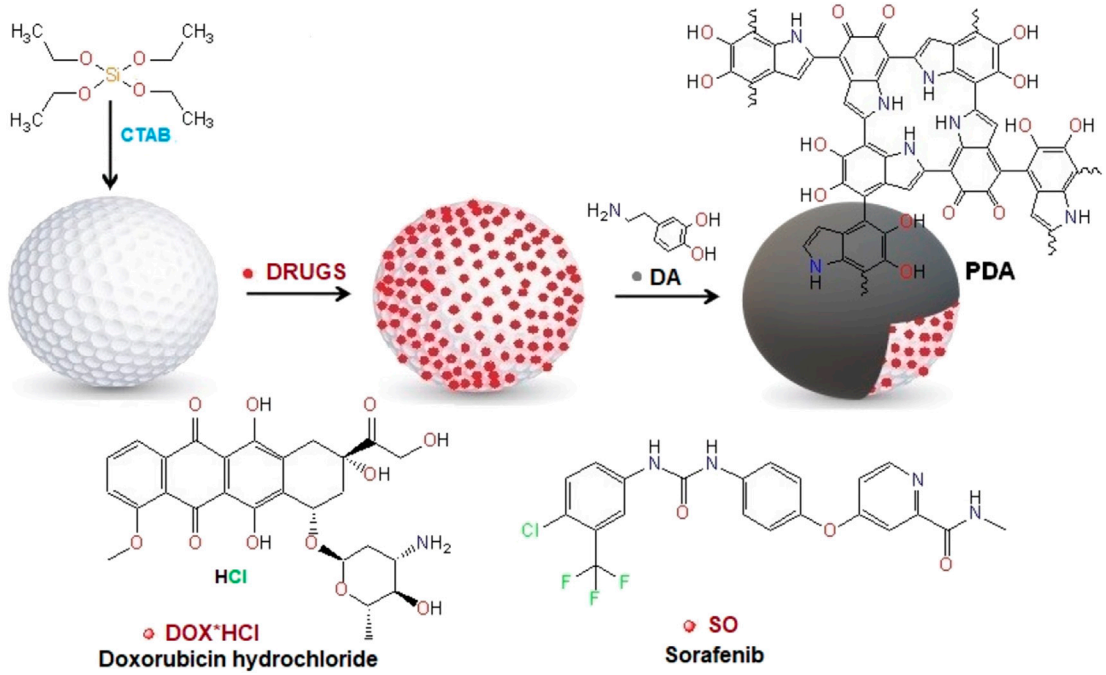

SCHEME 1
General scheme for the preparation of MSN@drug@PDA drug nanocarriers with the polydopamine coating.

stirring with addition of small molecules, e.g., H_2O_2 or GSH, mimicking the cancer cell environment. In this manner, we have made the first step toward a protocol allowing comparison of different carriers based on MSN and other porous structures with PDA coating and towards understanding the release behavior of the drugs, depending on the nature of the applied external stimuli. Thus, our results are of great importance for development of advanced nanocarriers based on mesoporous silica nanoparticles and provide important methodological information for design and development of other nanocarriers.

2 Results and discussion

2.1 Synthesis and characterization of nanoparticles

The procedure of MSN@drug@PDA fabrication is schematically illustrated in Scheme 1. At first, the MSN were prepared via a literature described sol–gel CTAB-templated method (Luo et al., 2011; Xie et al., 2013; Tang et al., 2019). The obtained materials were subjected to calcination to induce formation of mesoporous structures (Agostini et al., 2012). After synthesis, the nanoparticles were characterized by the zeta potential measurements of – 15 mV (Figures 1A, B), which were performed in MiliQ water with resistivity of 18.2 MΩ*cm. The morphology of bare MSNs was investigated by SEM imaging. The SEM analysis of MSNs revealed that the nanoparticles had spherical shape and were nearly 200 nm in diameter. Additionally, the TEM analysis confirmed that the nanoparticles were spherical (Figures 2A, B right inset). Successful removal of the surfactant CTAB from MSNs was corroborated by the disappearance of the C-H stretching vibration and C-H bending vibration assigned to CTAB, at 2,924, 2,853 and 1,489 cm^{-1} in the FTIR spectra of MSNs after calcination (Supplementary Figure S3). Additionally, we performed a BET analysis from which it is clearly visible the surface area of MSNs changed from 563 m^2/g to 910 m^2/g after CTAB removal (Supplementary Table S1). The anticancer drug DOX or SO was loaded into the mesopores of MSNs in via adsorption (Luo et al., 2011; Xie et al., 2013; Martínez-Carmona et al., 2015). The obtained nanoparticles were subjected to oxidative self-polymerization of dopamine under weak alkaline conditions to obtain MSN@drug@PDA according to a reported protocol (Zheng et al., 2014). Before loading the drugs, we checked whether the PDA formed a layer on the surface of the mesoporous silica. To confirm the formation of MSN@PDA, we perform a TEM image to show the PDA layer on mesoporous silica particles (Supplementary Figure S2). In addition, the BET analysis of MSN@PDA showed a decrease in the specific surface area from 910 m^2/g to 623 m^2/g, which confirms the coating of MSN by PDA, yielding a drop in the surface area.

In our experiments we chose DOX as a model anticancer drug as it is commonly applied in different anticancer therapies, including those of hepatocellular carcinoma and breast cancer. MSNs were loaded with DOX in a PBS buffer at pH 7.4. A neutral environment was employed to ensure equilibrium between DOX solubility and stability. The alkaline conditions might favor the entry of DOX into the mesoporous pores enhancing the loading capacity (LC) thanks to a better solubility of DOX. However, in the basic conditions more rapid degradation/dissolution of silica can occur, which can cause carrier degradation. (Beijnen et al., 1986). The UV-Vis spectroscopy was employed to determine the loading capacity of DOX which was above 66 wt%. The obtained LC was higher than those reported so

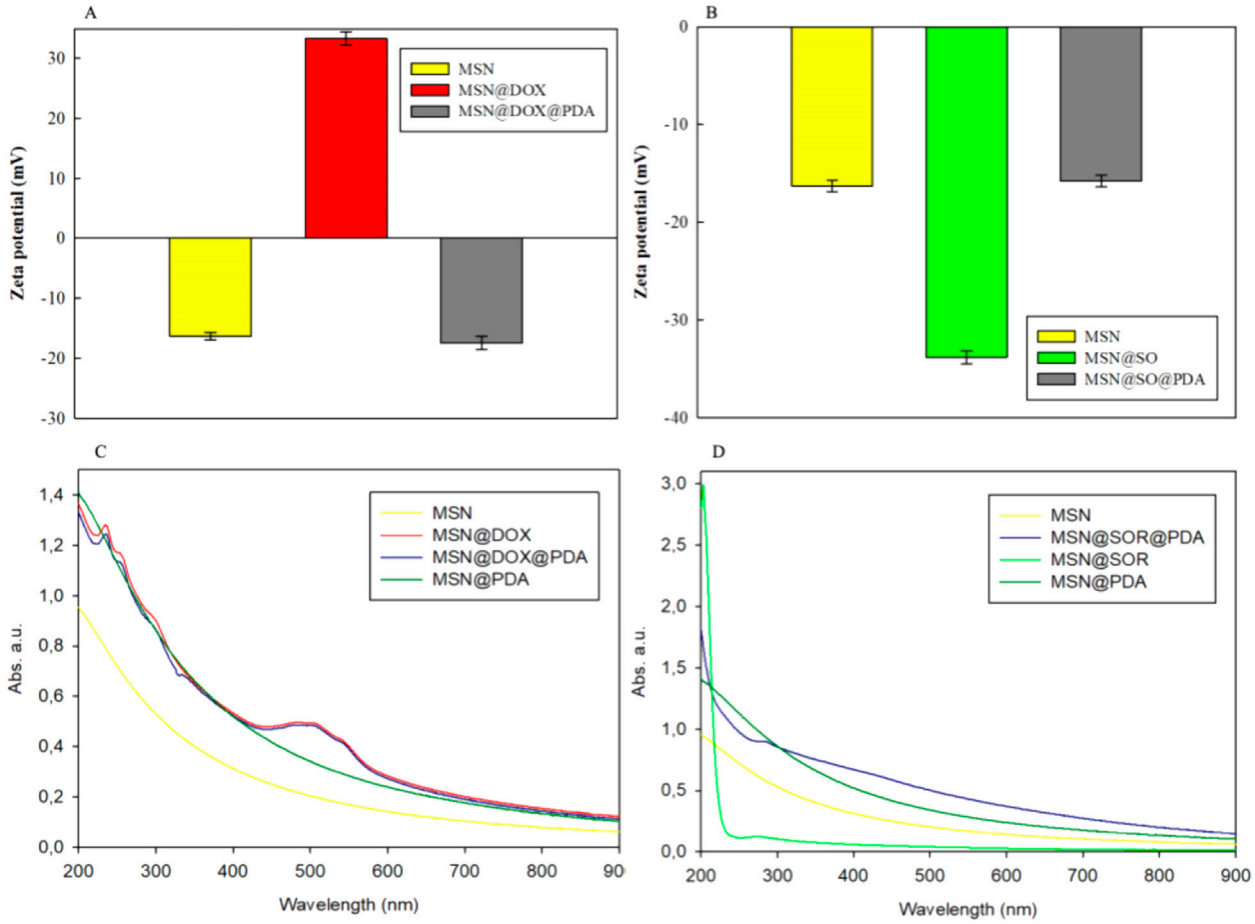

FIGURE 1
(A) Zeta potential of MSN; MSN@DOX; MSN@DOX@PDA, **(B)** Zeta potential of MSN; MSN@SO; MSN@SO@PDA, **(C)** UV-Vis spectrum of MSN; MSN@DOX; MSN@DOX@PDA and MSN@PDA, **(D)** UV-Vis spectrum of MSN; MSN@SO; MSN@SO@PDA and MSN@PDA.

far in literature (Chen et al., 2014; Martínez-Carmona et al., 2015; Li et al., 2015), giving LE in the range of 13.6 wt% - 44.3 wt%. However, comparison of loading efficiency to the results reported by other authors does not provide useful information since the loading is an adsorption-based process and thus, highly dependent on the initial drug concentration (i.e., full adsorption can be reached at lower concentrations, so a high LE does not automatically mean a high loading degree. The same is true for SO LE in further part of the text.

In the next step, we performed the FTIR analysis of MSN@DOX and MSN@DOX@PDA (Figure 3A) to identify the functional groups present in our materials and to check the loading of the anticancer drug and the PDA coating (Figure 3A). The spectra of MSN@DOX and MSN@DOX@PDA show characteristic bands at ~800 cm^{-1} and ~1,100 cm^{-1} that are assigned to Si-O-Si vibrations. The vibration band at about 960 cm^{-1} originates from the silanol groups (Si-OH) present in the silica nanoparticles. The intense signals at 1,323 cm^{-1}, 1,392 cm^{-1} arise due to the C-O, C-O ether groups of DOX. The bands at 1,613 cm^{-1}, 1722 cm^{-1}, 2,529 cm^{-1} are assigned to the C=C, C=O, -OH moieties in DOX. A wide band at about ~3,400–3,500 cm^{-1} corresponds to the Si-OH and -OH group from MSNs and DOX. After the coating of the nanoparticles with PDA, the FTIR spectrum was changed. The DOX loading on MSNs and PDA coating were also corroborated by a change in the zeta potential (Figure 1A) of bare MSNs from −15.7 ± 0.6 mV to +32.3 ± 0.8 mV for MSN@DOX and further to −18.6 ± 0.4 mV for MSN@DOX@PDA. Moreover, the UV-Vis spectrum of MSN@DOX-PDA shows a new peak 484 nm assigned to DOX, and was additional evidence of successful loading of DOX on MSNs (Figure 1C). Finally, SEM investigations of MSN@DOX and MSN@DOX@PDA showed that the particles retained the spherical structure and confirmed that PDA coating had insignificant effect on the particles size (Supplementary Figures S1B, C). It is worth highlighting that the loading of DOX and PDA coating was reflected by the color change of the materials. Solid MSNs were white, while after loading the particles changed color to brick red and further became dark brown after the modification with PDA coating.

Sorafenib is a small-molecule inhibitor of several tyrosine protein kinases, including VEGFR, PDGFR, and the Raf kinase family (Wilhelm et al., 2006). It inhibits tumour cell proliferation, angiogenesis and increases the apoptosis of a wide range of tumours (Chang et al., 2007). Moreover, it is approved for the treatment of advanced renal cell carcinoma, liver cancer, and radioactive iodine resistant advanced thyroid carcinoma. In our study, MSNs were loaded with SO in DMF since SO is insoluble in water. However, DMF can be easily removed by water extraction. The determined

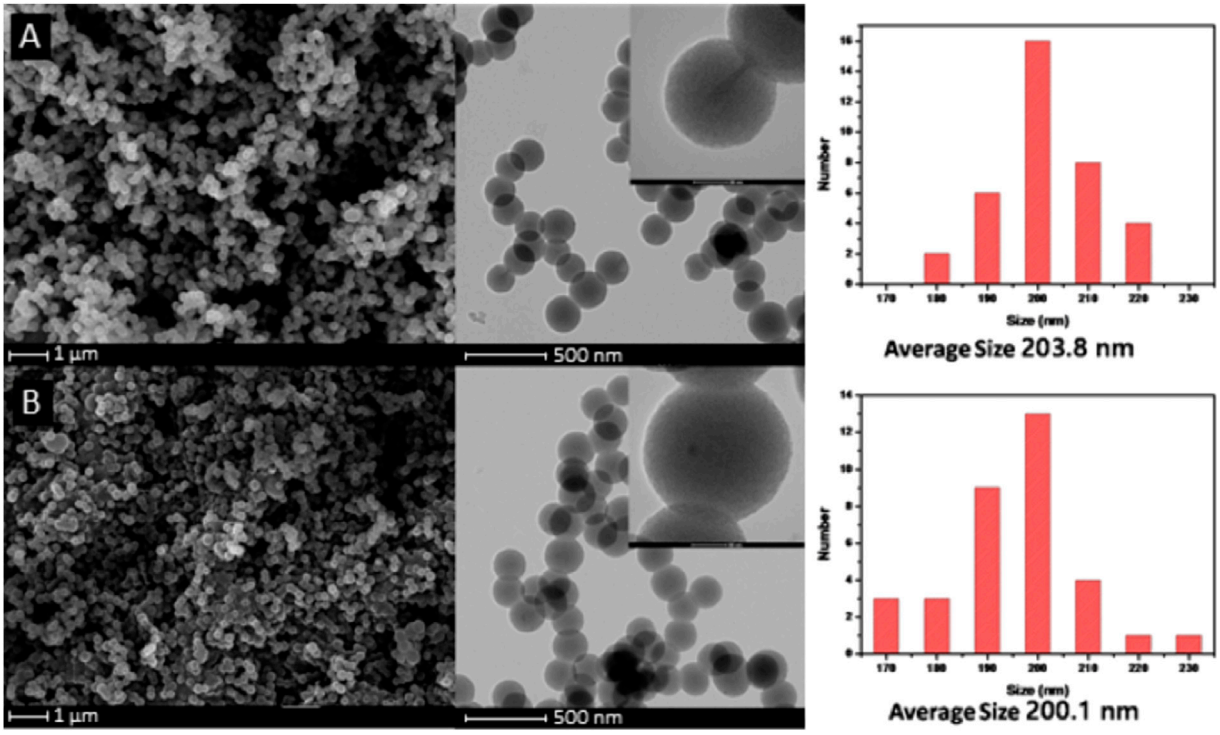

FIGURE 2
(A) TEM images of MSNs-CTAB and **(B)** MSNs.

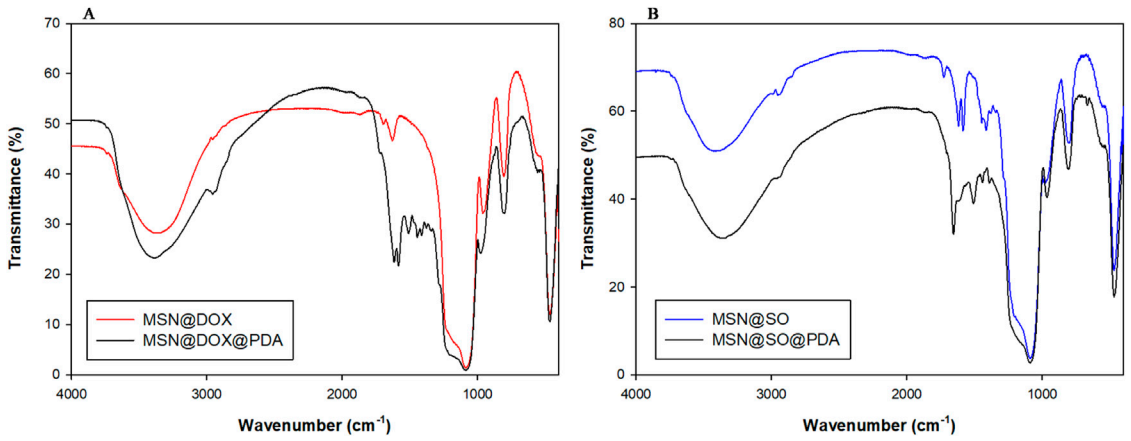

FIGURE 3
(A) FT-IR spectrum MSN@DOX and MSN@DOX@PDA, **(B)** FT-IR spectrum MSN@SO and MSN@SO@PDA.

loading capacity of SO was about 65.2 wt%. This value is higher than those reported so far of SO in MSNs of 2.68 wt% and 22.4 wt%. (Tang et al., 2019; Zheng et al., 2018). In contrast to DOX, the loading of SO molecules did not change the color of MSNs. However, after the PDA coating of MSN@SO the nanoparticles changed color to black. The FTIR spectra of MSN@SO and MSN@SO@PDA are shown in Figure 3B. Similarly to the spectra of the carrier with DOX, those of MSN@SO show bands at ~800 and ~1,100 cm^{-1} which are assigned to Si-O-Si vibrations. The vibration band at about 960 cm^{-1} originates from silanol groups (Si-OH). The stretching bands observed at 1,602 cm^{-1}, 1721 cm^{-1} (C=O stretch), 3,061 cm^{-1} were assigned to the functional groups from SO, such as carbonyl groups, or urea group. After the PDA coating, new absorption signals at 1,506 and 1,442 cm^{-1} appeared in the spectrum of MSN@SO@PDA and were assigned to the C=C resonance vibrations in the aromatic ring and the NH bending vibrations from PDA. A broad band of about ~3,400–3,500 cm^{-1} came from the -OH group in Si-OH catechol moieties. The SO loading on MSNs and PDA coating were also corroborated by a change in the zeta potential of MSNs from −15.7 ± 0.6 mV to −33.2 ± 0.7 mV for MSN@SO and further −15.2 ± 0.2 mV for MSN@SO@PDA (Figure 1B). UV-Vis spectroscopy provided

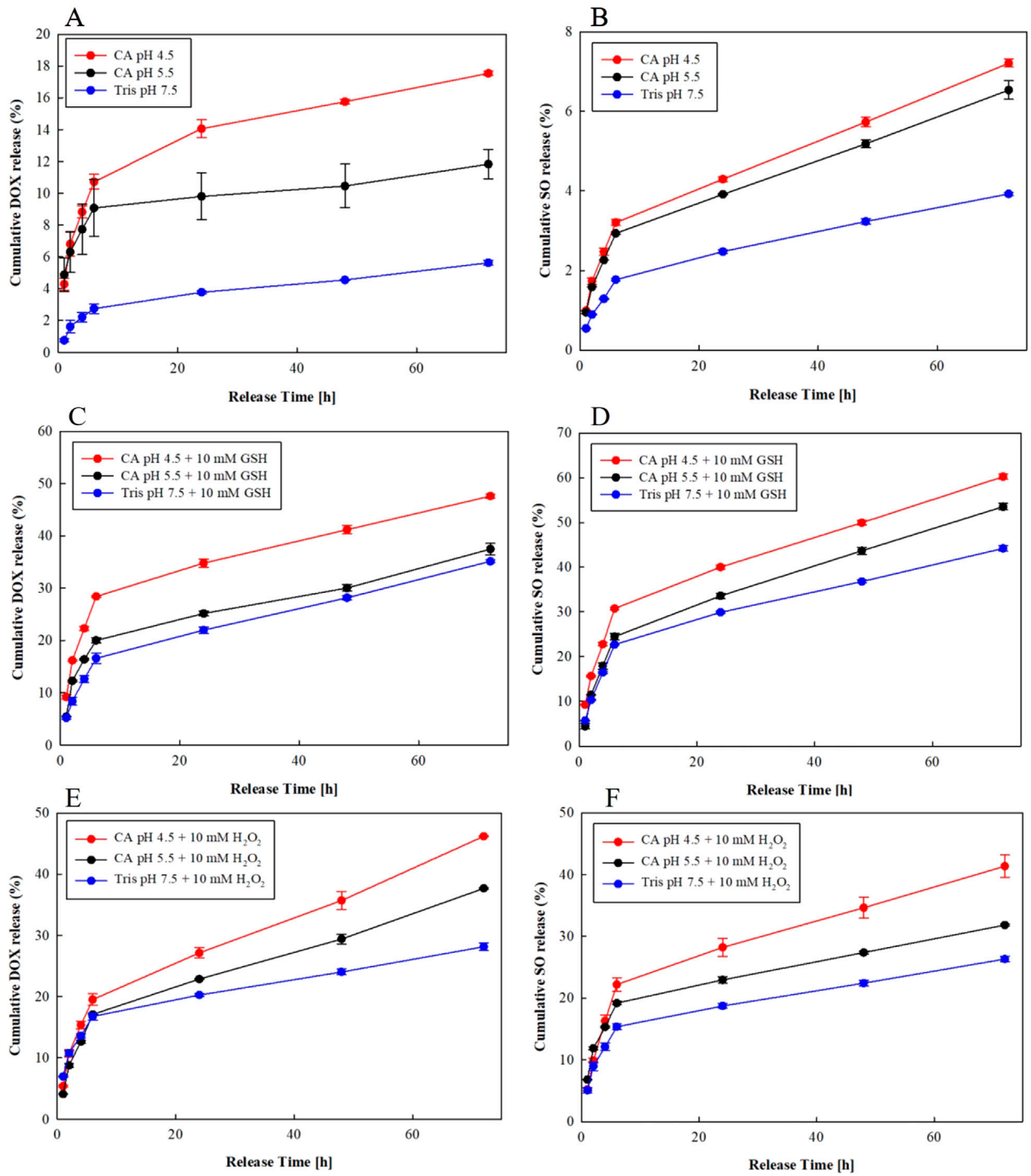

FIGURE 4
(A–C) DOX release kinetic curves from MSN@DOX@PDA in various environments obtained under stirring conditions, **(D–F)** SO release kinetic curves from MSN@SO@PDA in various environments obtained under stirring conditions.

additional evidence for SO loading on MSNs, which was the appearance of a new absorption peak at 264 nm in the spectrum of MSN@SO@PDA, not observed in the UV-Vis spectrum of MSN@PDA (Figure 1D). The SEM image of MSN@SO@PDA shows that the particles retained the spherical structure and their size also was not influenced by PDA coating (Supplementary Figures S1D, E).

2.2 Profile of DOX release from MSNs@DOX@PDA under different physiological conditions

DOX release from MSNs coated with PDA, used as carriers, was investigated at different pH from the range 4.5–5.5, with addition of GSH or H_2O_2 to mimic the environment found in cancer cells

(Swietach, 2019; Panieri and Santoro, 2016). We used two different procedures to study the drug release from our carriers. In the first one, we performed the release studies in a glass flask with a magnetic stirring bar, while in the second one, we were shaking the samples in a thermoblock. Surprisingly, the impact of these two procedures has never been compared even though they are often applied in different research works (Porciani et al., 2015; Hao et al., 2019). The lack of information about the impact of these actions on drug release precluded comparison of the performance of different carriers known in literature at the *in vitro* level. At first we tested the pH-triggered release of DOX from MSNs@DOX@PDA at different pH values including pH of 7.5, pH 5.5 and pH 4.5 using the stirring procedure in a glass flask at 37 °C. The amount of the drug in the supernatant was determined by UV-Vis spectroscopy using the standard calibration curve method (Supplementary Figure S4). It could be clearly noticed in Figure 4A that the decrease in pH value promoted the DOX release behavior since decreasing pH to 5.5 and 4.5 resulted in cumulative drug release of 10.9% and 17.4%, respectively, while at pH at 7.5 the cumulative drug release was only 5.5%. The increase in DOX release from the carriers at lower pH can be related to a combination of two factors. On the one hand, the solubility of DOX is inversely proportional to the pH value of solution, since DOX is protonated and converted into salt, which improves its solubility. On the other hand, in the acidic conditions, PDA to a certain extent suffers from degradation, which has been reported in literature (Li et al., 2018; Zheng et al., 2014) allowing penetration of the carriers by the buffer and release of the drug from the carrier.

Bearing in mind that cancer cells contain higher concentrations of GSH than healthy ones, which results in higher resistance to radio- or chemotherapy and to apoptosis (Karwicka, 2010), we decided to test the release of DOX from MSN@DOX@PDA at different pH levels with addition of 10 mM GSH. As shown in Figure 4C, the total amount of DOX released at pH 7.5 in the presence of 10 mM of GSH was 35.4%, while at pH 5.5 + 10 mM GSH and at pH 4.5 + GSH it was 38.5%, and 47.1%, respectively. In the performed tests we observed an approx. 20% increase in DOX release in the tested buffer solutions with the addition of GSH in relation to the same buffers without the GSH. This difference is well illustrated by the charts presented in Supplementary Figures S5A-C. This effect can be interpreted as a result of easier dissolution of the drug in the presence of GSH and an increase in the PDA surface degradation through gradual swelling of the polymer layer and formation of large cracks on the surface of the carrier through which the drug can freely escape (Hu et al., 2022; Li et al., 2015; Hao et al., 2019).

It has been reported that in the tumor microenvironment, hydrogen peroxide is present, which is often responsible for formation of reactive oxygen species (ROS) (Wang et al., 2016; Noh et al., 2015; Gisbert-Garzarán and Vallet-Regí, 2021). H_2O_2 could oxidize the phenols in the PDA to quinone, thereby weakening or even breaking the interaction between DOX molecules and PDA, while DOX and PDA interact with each other via π-π interactions and/or hydrogen bonding. Thus, we decided to carry out the DOX release experiments in the presence of H_2O_2 to determine the influence of hydrogen peroxide on DOX release from the nanocarrier (Yang et al., 2020). The obtained data are presented in Figure 4E. The addition of 10 mM of H_2O_2 increased the DOX release from 5.5% to about 27% at pH 7.5, from 10% to about 37% at pH 5.5 and from 17% to about 46% at pH 4.5, proving that H_2O_2 presence facilitates the DOX release from the carriers probably by weakening the π-π interaction as well as hydrogen bonding between PDA and DOX. Moreover, the PDA degradation under the applied conditions cannot be excluded.

It is worth emphasizing, that the level of DOX release from the MSN@DOX@PDA carrier in the presence of 10 mM H_2O_2 in most cases was slightly lower than the release in the environment supplemented with 10 mM GSH. The data are summarized in Supplementary Figure S5A-C. Nevertheless, the performed tests proved that DOX release from nanocarriers based on MSN is pH dependent and can be enhanced either by addition of GHS or hydrogen peroxide.

In the next step we performed the same tests but we replaced the glass flask with a small eppendorf tubes and applied shaking in a thermoblock without magnetic stirring. In this way, we wanted to answer the question if the method of drug release had any effect on the release efficiency. The graphs showing the DOX release from MSN@DOX@PDA with the use of shaking are summarized in Supplementary Figures S6A-F. In general, when comparing the kinetics of DOX release under different pH conditions and with different additives using stirring or shaking, we find that their course is analogous. In order to better visualize the total percentage of DOX released using stirring *versus* shaking at different pH and additive levels, the total value of the released drug after 48 h was chosen as a benchmark (Figure 5A). As can be seen in Figure 5A and in Supplementary Table S2, the difference in the total quantitative release of DOX after 48 h from the carrier under stirring *versus* shaking is within 4.4%.

2.3 Profile of SO release MSN@DOX@PDA under different physiological conditions

The SO release profile from MSN@SO@PDA was determined at the same pH values, as for DOX. Standard calibration curves for SO required for release determination are presented in Supplementary Figure S7 in Supporting Information. Also for studying the release of SO we stirred the samples using a stirring bar in the flasks at pH 4.5 and pH 5.5, which resulted in the drug release at 7% and 6%, respectively. However, almost no SO was released at pH 7.4 (Figure 4B), which makes MSN@SO@PDA a suitable carrier for SO delivery into tumour cells without premature leakage of the drug under physiological conditions and in the blood. After the addition of 10 mM GSH to the buffers, we observed a nearly 50% increase in SO release. As shown in Figure 4D, 60% of SO was released at pH 4.5 with addition of 10 mM GSH. At pH 5.5 + 10 mM GSH and pH 7.5 + 10 mM GSH, 53% and 43% of SO was released, respectively. This large increase in SO release in comparison to that observed in the variant without GSH, is a consequence of two factors. First of all, as mentioned earlier, GSH induces degradation of the PDA surface which protects the drug from leaking. Previous studies have demonstrated that GSH could destroy the aromatic ring of the oxidized PDA products (Dembereldorj et al., 2012; Kim et al., 2013), which may lead to a disruption of the π-π stacking interactions between PDA and SO. Secondly, GSH may facilitate the dissolution of SO in the buffer solution as already reported in literature (Tang et al., 2019; Geng et al., 2016).

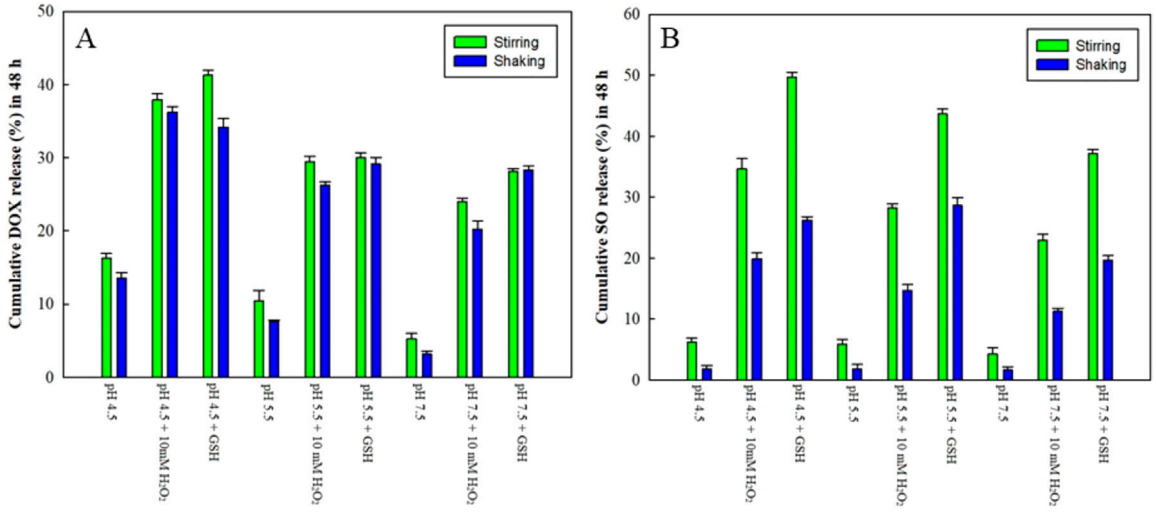

FIGURE 5
(A) Comparison of total DOX release after 48 h using stirring and shaking. **(B)** Comparison of total SO release after 48 h using stirring and shaking.

Also, for SO we tested the drug release from MSN@SO@PDA in buffers of varying pH with the addition of 10 mM H_2O_2, upon stirring the samples in the flasks. In a buffer solution at pH 4.5 + 10 mM H_2O_2, 39.5% of the drug was released, while at pH 5.5 + 10 mM H_2O_2, and at pH 7.5 + 10 mM H_2O_2 only 32% and 25.8%, (Figure 4F). As in previous experiments, we observed a decrease in the total SO release with increasing pH value. The release data are collected in Supplementary Figures S8A-C. The data analysis revealed that the SO release from the carriers is strongly enhanced by the addition of GSH rather than hydrogen peroxide (62%–43% depending on the pH of the buffer). Importantly, almost no release of SO was observed without the additives responsible for PDA degradation and interaction disruption, which is supported by recent literature reports (Guan et al., 2020; Zheng et al., 2018; Mokhtari et al., 2020).

In the last stage, the SO release was studied using a thermoblock. The graphs showing the results of SO release from the nanocarrier are presented in Supplementary Figures S9A-F. In general, the courses of the kinetics of SO release under different pH conditions and with different additives, using stirring or shaking were analogous. The greatest amount of SO was released in an acidic environment with the addition of 10 mM GSH (pH 4.5, 32.5%; pH 5.5, 36.1%), followed by a slight decrease in the release at pH 7.5 with 10 mmol GSH to 22.6% (Supplementary Figure S9B). After introduction of 10 mM H_2O_2 as an additive to the release medium, only approx. 10% of SO was released from the nanoparticles, which was less than when GSH was used (Supplementary Figure S9C). Moreover, the presence of the additives proved crucial for SO release, as without them the SO release was negligible and reached 2% (Supplementary Figure S9A).

To better visualize the total percentage of SO released upon stirring or shaking at different pH and additive levels, the cumulative release of the drug after 48 h was chosen as a benchmark (Figure 5B). As can be seen in Figure 5B and Supplementary Table S3, the difference in the release of SO after 48 h from the carrier using stirring or shaking ranged from 2.1% to 23.7% depending on the applied conditions. The smallest differences between the SO release from MSN@SO@PDA upon stirring and shaking were observed when the experiment was conducted in the buffers of pH 4.5, 5.5 and 7.5 without additives, they ranged from 2.1% to 4.4%. Much more significant differences between the SO release upon stirring or shaking were observed when H_2O_2 and GSH were added to the buffers of pH 4.5, 5.5 and 7.5. They ranged from 11.3% to 14% for 10 mM H_2O_2, and from 13.1% to 23.7% for 10 mM GSH.

2.4 Kinetic model and statistical analysis of the release profiles

In order to determine the DOX and SO release kinetics, the obtained data were fitted to different kinetic models such as zero-order, first-order, Higuchi's model, Korsmeyer-Peppas model, and Hixson-Crowell model. The correlation coefficient was calculated to define the approximation accuracy of each model and the results are shown in Tables 1, 2.

The highest values of R^2 were noted for Higuchi model in the case of MSN@DOX@PDA when the drug release studies were performed at pH 4.5 + 10 mM H_2O_2 under stirring conditions. However, at pH 4.5; 5.5; 7.5 and pH 4.5; 5.5; 7.5 with the addition of GSH and at pH 4.5; 5.5 with the addition of H_2O_2, the R^2 value was slightly lower. However, in all investigated environments, the R^2 value close to one corresponded to the Higuchi release model regardless of whether stirring or shaking was used. As for the previous DOX system, the highest R^2 values for MSN@SO@PDA release at different pH 4.5; 5.5; 7.5 and with additions of GSH and H_2O_2 corresponded to the Higuchi model. Regardless of the release method, stirring or shaking, the MSN@SO@PDA system works according to the Higuchi model. Higuchi model as mentioned earlier describes the release of drugs from an insoluble matrix as a square root of a time-dependent process based on Fickian diffusion. Moreover, the Higuchi model indicates that our delivery system exhibits the highest concentration of the released drug at the initial stage of the process, and then the equilibrium state is established (Dash et al., 2010; Paarakh et al., 2019; Singhvi and Singh, 2011).

TABLE 1 Kinetic models used to describe the release of Doxorubicin (DOX) from materials obtained.

Receptor medium	Zero- order	First- order	Higuchi	Hixson- Crowell	Korsmeyer- Peppas	
Stirring	R^2					*n*
pH 4.5	0.820	0.835	0.941	0.830	0.927	0.320
pH 4.5 + 10 mM H_2O_2	0.914	0.950	0.970	0.940	0.900	0.344
pH 4.5 + 10 mM GSH	0.800	0.857	0.932	0.839	0.907	0.441
pH 5.5	0.800	0.832	0.941	0.828	0.907	0.216
pH 5.5 + 10 mM H_2O_2	0.905	0.935	0.965	0.926	0.924	0.448
pH 5.5 + 10 mM GSH	0.841	0.882	0.923	0.869	0.882	0.375
pH 7.5	0.805	0.809	0.895	0.809	0.809	0.391
pH 7.5 + 10 mM H_2O_2	0.856	0.880	0.946	0.872	0.941	0.291
pH 7.5 + 10 mM GSH	0.894	0.923	0.959	0.914	0.950	0.395
Receptor medium	Zero- order	First- order	Higuchi	Hixson- Crowell	Korsmeyer- Peppas	
Shaking	R^2					*n*
pH 4.5	0.775	0.789	0.905	0.784	0.895	0.337
pH 4.5 + 10 mM H_2O_2	0.848	0.894	0.926	0.880	0.898	0.343
pH 4.5 + 10 mM GSH	0.783	0.837	0.878	0.820	0.832	0.457
pH 5.5	0.679	0.690	0.809	0.686	0.659	0.688
pH 5.5 + 10 mM H_2O_2	0.868	0.899	0.935	0.889	0.887	0.401
pH 5.5 + 10 mM GSH	0.835	0.873	0.917	0.861	0.866	0.369
pH 7.5	0.875	0.875	0.948	0.877	0.944	0.372
pH 7.5 + 10 mM H_2O_2	0.908	0.925	0.969	0.919	0.962	0.403
pH 7.5 + 10 mM GSH	0.770	0.804	0.892	0.793	0.880	0.409

R^2, correlation coefficient; n, release exponent.

Finally, to check whether the differences observed by us in the release of DOX and SO drugs, depending on the application of stirring or shaking, are statistically significant, we determined the two fit factors: the difference factor (f_1) and the similarity factor (f_2) of drug release profiles, using the DDSolver software. It should be noted that these factors have been adopted by the Centre for Drug Evaluation and Research (FDA) and by Human Medicines Evaluation Unit of The European Agency for the Evaluation of Medicinal Products (EMEA), as criteria for the assessment of similarity between two *in vitro* dissolution profiles. These factors were also reported in the "Guidance on Immediate Release Solid Oral Dosage Forms; Scale-up and Post approval Changes: Chemistry, Manufacturing, and Controls; *In Vitro* Dissolution Testing; *In Vivo* Bioequivalence Documentation" (Shah et al., 1998; Hermans et al., 2017). Comparison of the release profiles of an API from a drug formulation is used as a standard in the pharmaceutical industry at the stage of preparing a new formulation, and then in generic drug bioequivalence studies. For the first time, we used the comparison of the release profiles of 2 drugs (DOX and SO) from the same matrix under different release conditions at the initial stage of basic research. The purpose of this comparison was to check whether the conditions under which the release of the active substance is carried out, affect the level of the release of the drug from the mesoporous matrix. The results of the statistical calculations are presented in Tables 3, 4 for DOX and SO, respectively. As noted in the section on statistical calculations, in order to consider dissolution profiles as similar, the f_1 values should be close to 0 and values of f_2 should be close to 100. In general, f_1 values lower than 15 (0–15) and f_2 values higher than 50 (50–100) point to similarity of the dissolution profiles (Samaha et al., 2009). In practice, the calculated similarity factor values show that the differences between the release profiles at individual time points do not exceed 10%.

Analysis of the statistical results obtained for DOX release curves by stirring or shaking showed that the f_1 and f_2 factors perform the values $f_1 > 15$ and $f_2 > 50$, respectively, for the release media characterized by pH 4.5; pH 4.5 + 10 mM GSH; pH 5.5; pH 7.5 and pH 7.5 + 10 mM H_2O_2 (Table 3). The results revealed that the release curves for all parameters are similar only in terms of similarity (f_2) but they are different for the difference terms (f_1). It is worth noting that the coefficient f_2 assumes the true value in a wide range of 50–100. The f_2 values for DOX are in range from 59.4 (pH 4.5 + 10 mM GSH) to 92.74 (pH 7.5 + 10 mM GSH). Despite the wide spread, the assumptions for the coefficient f_2 are met for all these values. Therefore, we have

10.3389/frcdi.2025.1531144

TABLE 2 Kinetic models used to describe the release of Sorafenib (SO) from materials obtained.

Receptor medium	Zero- order	First- order	Higuchi	Hixson- Crowell	Korsmeyer- Peppas	
Stirring	R^2					*n*
pH 4.5	0.927	0.931	0.975	0.930	0.963	0.419
pH 4.5 + 10 mM H_2O_2	0.848	0.890	0.935	0.877	0.912	0.429
pH 4.5 + 10 mM GSH	0.879	0.941	0.955	0.923	0.941	0.399
pH 5.5	0.909	0.913	0.968	0.912	0.953	0.405
pH 5.5 + 10 mM H_2O_2	0.819	0.852	0.916	0.841	0.915	0.314
pH 5.5 + 10 mM GSH	0.890	0.942	0.961	0.927	0.887	0.520
pH 7.5	0.917	0.920	0.977	0.918	0.966	0.423
pH 7.5 + 10 mM H_2O_2	0.835	0.860	0.925	0.852	0.916	0.352
pH 7.5 + 10 mM GSH	0.860	0.905	0.945	0.890	0.926	0.430
Receptor medium	Zero- order	First- order	Higuchi	Hixson- Crowell	Korsmeyer- Peppas	
Shaking	R^2					*n*
pH 4.5	0.857	0.853	0.937	0.857	0.930	0.360
pH 4.5 + 10 mM H_2O_2	0.873	0.892	0.950	0.886	0.935	0.393
pH 4.5 + 10 mM GSH	0.887	0.915	0.959	0.906	0.947	0.398
pH 5.5	0.867	0.865	0.947	0.866	0.932	0.400
pH 5.5 + 10 mM H_2O_2	0.872	0.887	0.952	0.882	0.924	0.423
pH 5.5 + 10 mM GSH	0.883	0.914	0.957	0.904	0.949	0.385
pH 7.5	0.881	0.884	0.951	0.883	0.937	0.375
pH 7.5 + 10 mM H_2O_2	0.874	0.885	0.949	0.881	0.930	0.397
pH 7.5 + 10 mM GSH	0.866	0.886	0.947	0.880	0.934	0.383

R^2, correlation coefficient; n, release exponent.

TABLE 3 The fit factors f_1 and f_2 of Doxorubicin (DOX) release profiles.

Medium	f_1	f_2
pH 4.5	17.6	84.25
pH 4.5 + 10 mM H_2O_2	14.43	75.17
pH 4.5 + 10 mM GSH	24.02	59.40
pH 5.5	34.06	79.27
pH 5.5 + 10 mM H_2O_2	7.81	82.46
pH 5.5 + 10 mM GSH	6.12	88.53
pH 7.5	40.24	89.97
pH 7.5 + 10 mM H_2O_2	30.05	66.55
pH 7.5 + 10 mM GSH	5.29	92.74

TABLE 4 The fit factors f_1 and f_2 of Sorafenib (SO) release profiles.

Medium	f_1	f_2
pH 4.5	75.90	77.80
pH 4.5 + 10 mM H_2O_2	41.96	52.40
pH 4.5 + 10 mM GSH	47.22	41.21
pH 5.5	76.44	79.32
pH 5.5 + 10 mM H_2O_2	56.16	49.37
pH 5.5 + 10 mM GSH	33.48	57.59
pH 7.5	63.50	89.99
pH 7.5 + 10 mM H_2O_2	54.09	55.40
pH 7.5 + 10 mM GSH	46.12	48.25

determined the difference factor f_1, which is varying in the narrower range of 0–15. In this case, most of the release profiles are no longer similar (f_1 > 15). Cumulatively, these results indicate that DOX release profiles obtained by stirring or shaking in most of the used media (5 out of 9) are statistically different, which proves the importance of the mode of drug release tests performance. We then analyzed the statistical data obtained for the SO release under stirring or shaking (Table 4). Parameter f_1 was >15 for all assessed release curves, whereas the parameter f_2 was <50 for the media characterized by pH 4.5 + 10 mM GSH; pH 5.5 + 10 mM H_2O_2 and

pH 7.5 + 10 mM GSH and for the other media - $f_2 > 50$. These results show that the SO release profiles obtained upon shaking or stirring in all media are statistically different and again confirmed a crucial effect of the mode of drug release tests performance.

3 Materials and methods

3.1 Materials

Tetraethyl orthosilicate (TEOS) (99.0%, Sigma), sodium hydroxide (NaOH, Stanlab), Hexadecyltrimethylammonium bromide (CTAB) (95%, Sigma), ammonium hydroxide solution (28.0%–30.0%, Sigma), ethyl alcohol anhydrous (99.9%, Daejung) and ethylene glycol (EG) were purchased from Aldrich. Doxorubicin hydrochloride (DOX, 98%) was supplied by Apollo Scientific Company. Sorafenib (SO) was supplied by Angene Chemical Company. DopamineHCl (DOPA) was provided by Fluorochem. Trizma base and, phosphate buffered saline tablet were supplied by Aldrich Poland. Citric acid, sodium citrate, dimethylformamide, and hydrogen peroxide solution (H_2O_2) were purchased from POCH S.A. (Avantor Performance Materials Poland). All solvents (GR grade) were used without further purification.

3.2 Synthesis of mesoporous silica nanoparticles (MSN)

The synthesis of MSNs was performed according to the described procedure with slight modifications (Luo et al., 2011; Xie et al., 2013; Beijnen et al., 1986). Mesoporous SiO_2 (MSN) was synthesized by the modified Stöber method. Three mM of hexadecyltrimethylammonium bromide (CTAB) in 600 mL of DI water were stirred for 30 min at 40°C. Then, 250 mL of ethyl alcohol and 4.7 mL of ammonium hydroxide solution were added to the above solution and the contents were stirred for 5 min. Next, 4.7 mL of tetraethyl orthosilicate (TEOS) were added dropwise and the contents were stirred for 48 h at 60 °C. After cooling the above solution to room temperature, it was washed with ethanol using a filter of 0.22 μm. The resulting solid MSNs were dried in an oven at 60 °C overnight. For the CTAB removal, 2 g of MSNs was placed in a tube furnace at 600 °C for 4 h in air atmosphere.

3.3 Synthesis of mesoporous silica nanoparticles covered with polydopamine (MSN@PDA)

MSNs (150 mg) were ultrasonically dispersed in 200 mL Tris buffer (10 mM, pH 8.5) for 10 min. Next, dopamine hydrochloride (100 mg) was added into the MSNs@drug dispersion and the suspension was stirred continuously for 18 h at 25 °C. In the next step, the mixture was centrifuged and washed with the Tris buffer of pH 8.5 (1 × 10 mL) and MilliQ water (3 × 10 mL). Finally, the products were suspended in water and stored for up to before use.

3.4 Loading drugs on MSNs

3.4.1 Loading of DOX on MSN

DOX (10.4 mg) was dissolved in 10 mL PBS buffer solution (10 mM, pH 7.4) at RT using ultrasounds (US) for 5 min. Subsequently, MSNs (5 mg) were ultrasonically dispersed in the solution, and the mixture was magnetically stirred at 25°C for 24 h. To remove the physically adsorbed DOX, the obtained MSN@DOX particles were collected by centrifugation and gently washed with the MilliQ water until no signal of DOX was as observed in the supernatant. Finally, the products were suspended in water and stored for up to 1 day before use. The amount of DOX loaded on the MSN@DOX was determined by a UV–Vis spectrophotometry at 486 nm, using the standard calibration curve method.

3.4.2 Loading of SO on MSN

SO (10.4 mg) was dissolved in 10 mL DMF at RT using US, for 5 min. Subsequently, MSNs (5 mg) were ultrasonically dispersed in the solution, and the mixture was magnetically stirred at 25 °C for 24 h. To remove the physically adsorbed SO, the resulting MSNs@SO particles were collected by centrifugation and gently washed with the MilliQ water until no signal of SO was as observed in the supernatant. Finally, the products were suspended in water and stored for up to 1 day before use. The amount of SO loaded on the MSN@SO was determined by a UV–Vis spectrophotometry at 264 nm using the standard calibration curve method. The minimum amount of DMF was necessary to increase solubility of SO in water medium and to measure the UV spectra. The supernatant was not transparent but it become clearer after addition of DMF.

The drug loading capacity was calculated using the following formula:

$$loading\ capacity\ (wt.\%) = \frac{mass\ of\ total\ drug - mass\ of\ drug\ in\ supernatant}{mass\ of\ total\ drug\ carrier} \times 100\%$$

3.5 Preparation of polydopamine coated MSN@drug particles

MSN@drug (DOX or SO) (15 mg) particles were ultrasonically dispersed in 20 mL Tris buffer (10 mM, pH 8.5) for 10 min. Next, dopamine hydrochloride (10 mg) was added to the MSNs@drug dispersion and the suspension was stirred continuously for 18 h at 25°C. In the next step, the mixture was centrifuged and washed with the Tris buffer of pH 8.5 (1 × 10 mL) and MilliQ water (3 × 10 mL). Finally, the products were suspended in water and stored for up to 1 day before use.

3.6 Drug release from MSN@drug@PDA carriers under different physiological conditions

Briefly, 2 mg of MSN@drug@PDA (DOX or SO) were mixed with 2 mL of appropriate buffer (citric buffer (CA) (10 mM, pH =

4.5); citric buffer (10 mM, pH = 4.5) with 10 mM GSH; citric buffer (10 mM, pH = 4.5) with 10 mM H_2O_2; citric buffer (10 mM, pH = 5.5); citric buffer (10 mM, pH = 5.5) with 10 mM GSH; citric buffer (10 mM, pH = 5.5) with 10 mM H_2O_2; Tris buffer (10 mM, pH = 7.5); Tris buffer (10 mM, pH = 7.5) with 10 mM GSH; Tris buffer (10 mM, pH = 7.5) with 10 mM H_2O_2 respectively) at 37 °C to determine the effect of pH and the additives on the character of the drug release. The, samples were collected at various time intervals (1, 2, 4, 6, 24, 4 and 72 h) and the mixture was refilled with a fresh buffer portion. To evaluate the impact of shaking and stirring on drug release from the carrier, we conducted tests using a 5 mL flask and a 2 mL tube. The samples subjected to magnetic stirring were thermostated in an oil bath at 37°C, ensuring consistent temperature control during the process. On the other hand, the shaking experiments were performed in a thermoblock equipped with precise temperature control, also set to 37°C. Both stirring and shaking were carried out at a speed of 360 rpm The amount of released drug in the supernatants was evaluated in all experiments by UV-Vis spectroscopy at 486 nm for DOX and at 264 nm for SO.

All experiments were performed threefold for all samples. The results of active ingredient release were averaged and expressed as mean ± standard deviation. Next, they were fitted to five different mathematical models such as zero-order (% drug release vs time), first-order (log of % drug remaining vs time), Higuchi's model (% drug release vs square root of time), Korsmeyer-Peppas model (log of % drug release vs log time) and Hixson-Crowell model (cube root of % of drug remaining vs. time) in order to analyze the kinetics and the mechanism of the process (Samaha et al., 2009; Chen et al., 2014; Martínez-Carmona et al., 2015; Li et al., 2015). To assess the fit to each presented model was characterized by the calculated correlation coefficient (R^2).

3.7 Statistical calculations

The difference factor (f_1) and similarity factor (f_2) for the Doxorubicin and Sorafenib release profiles from MSN@DOX@PDA, obtained under different physiological conditions were determined using the DDSolver software (Zhang et al., 2010). The factor f_1 is the average percentage difference over all time points in the amount of DOX or SO dissolved by shaking (test profile) as compared to the DOX or SO dissolved by stirring (reference profile). The f_1 values for the test and the reference profiles are identical and increase proportionally with the dissimilarity between the two profiles. The f_2 value is between 0 and 100 it takes the value of. The f_2 value is 100 when the test and the reference profiles are identical and approaches 0 as the dissimilarity increases (Anderson et al., 1998).

3.8 Characterization methods

The morphology of nanomaterial flakes was examined by scanning electron microscopy (SEM) Quanta 250 FEG, FEI. Samples were drop-casted on a silicon wafer. Fourier transform infrared (FT-IR) spectra were recorded on a NicoletiS 50 spectrometer in KBr pellets. Zeta potentials were measured using Zetasizer Nano ZS (Malvern Instruments Ltd., Malvern). UV-Vis absorption spectra of nanoparticles (MSN; MSN@DOX; MSN@DOX@PDA; MSN@PDA; MSN@SO and MSN@SO@PDA) and released drugs (DOX and SO) were measured on a UV-Vis spectrometer (Nicolet Evolution 220 PC). The morphology and crystallinity of the obtained materials were determined using Transmission Electron Microscopy (JEOL JEM 1200EX II), Field-Emission Scanning Transmission Electron Microscopy (JEOL JSM-7610F) and Field-Emission Scanning Electron Microscopy (Thermo Fisher Scientific Talos F200X). FT-IR spectrophotometer (Agilent Technologies Cary 610/660) was used to analyze the surrounding functional groups. The specific surface area was calculated on the basis of the nitrogen adsorption-desorption isotherms at 77 K by BET method (Micromeritics Co. ASAP 2020).

4 Conclusion

In this paper, we presented results of extensive studies on drugs release profiles of two, different in nature, anticancer drugs: hydrophilic DOX hydrochloride or hydrophobic sorafenib from mesoporous silica particles coated with polydopamine. Both systems showed high drug loading capacity and their release could be triggered by applying different pH and additives such as GSH and H_2O_2. The highest release efficiency of DOX and SO, was found to take place in a citrate buffer of pH 4.5 with the addition of 10 mM GSH. Importantly, we have proved that there is a statistical difference in the release of SO and DOX depending not only on the release medium and the presence of additives, but also on the applied mode of release tests (stirring vs. shaking). The release of both DOX and SO from the carrier was best described by the Higuchi kinetics model, in all tested conditions. It is worth highlighting, that in the case of DOX, both GSH and H_2O_2 could promote the drug release from the carrier at almost the same level, while in the case of SO, the presence of GSH had greater influence on cumulative release of the drug from the carrier. In both cases the higher cumulative release of both drugs was achieved under stirring conditions. Therefore, our studies point out that it is important to know the agitation mode to compare drug release results of different studies The presented results are important for development of nanocarriers based on mesoporous silica nanoparticles and polydopamine. as well as for progress in the field of nanomedicine, as we have provided evidence of the effect of the mode of stirring (stirring or shaking) on drug release behavior that should be taken under consideration comparing the release of entrapped drugs from the nanocarriers reported from different studies. This also a crucial aspect for standardization of drug release from nanocarriers and their future upscaling from the laboratory to pharmaceutical industry.

Indeed, one cannot compare the conditions applied in our *in vitro* tests with those present *in vivo*. We suppose that the stirring mode is more appropriate since the forces generated upon during stirring may be compared with those forces exerted on to carriers in the blood flow. It is also known that nanocarriers may stuck in the cells and then the chemical conditions, e.g., pH or the presence of an additive may govern the drug release.

Data availability statement

The original contributions presented in the study are included in the article/Supplementary Material, further inquiries can be directed to the corresponding author.

Author contributions

SO: Formal Analysis, Conceptualization, Investigation, Methodology, Visualization, Writing–original draft, Writing–review and editing. MS: Investigation, Visualization, Writing–review and editing. SK: Investigation, Visualization, Writing–original draft. YK: Investigation, Visualization, Writing–review and editing. DW: Writing–original draft, Formal Analysis. RM: Formal Analysis, Conceptualization, Funding acquisition, Methodology, Project administration, Resources, Supervision, Writing–review and editing.

Funding

The author(s) declare that financial support was received for the research, authorship, and/or publication of this article. The financial support of the National Science Centre (NCN) under the OPUS program UMO-2018/31/B/ST8/02460 is acknowledge.

Conflict of interest

The authors declare that the research was conducted in the absence of any commercial or financial relationships that could be construed as a potential conflict of interest.

Generative AI statement

The author(s) declare that no Generative AI was used in the creation of this manuscript.

Publisher's note

Supplementary material

The Supplementary Material for this article can be found online at: https://www.frontiersin.org/articles/10.3389/frcdi.2025.1531144/full#supplementary-material

References

Agostini, A., Mondragõn, L., Bernardos, A., Martínez-Máñez, R., Marcos, M. D., Sancenõn, F., et al. (2012). Targeted cargo delivery in senescent cells using capped mesoporous silica nanoparticles. *Angew. Chem. - Int. Ed.* 51 (42), 10556–10560. doi:10.1002/ANIE.201204663

Anderson, N. H., Bauer, M., Boussac, N., Khan-Malek, R., Munden, P., and Sardaro, M. (1998). An evaluation of fit factors and dissolution efficiency for the comparison of *in vitro* dissolution profiles. *J. Pharm. Biomed. Analysis* 17 (4–5), 811–822. doi:10.1016/S0731-7085(98)00011-9

Ashley, C. E., Carnes, E. C., Phillips, G. K., Padilla, D., Durfee, P. N., Brown, P. A., et al. (2011). The targeted delivery of multicomponent cargos to cancer cells by nanoporous particle-supported lipid bilayers. *Nat. Mater.* 10 (5), 389–397. doi:10.1038/nmat2992

Barba, A. A., Dalmoro, A., D'Amore, M., Vascello, C., and Lamberti, G. (2014). Biocompatible nano-micro-particles by solvent evaporation from multiple emulsions technique. *J. Mater. Sci.* 49 (14), 5160–5170. doi:10.1007/s10853-014-8224-1

Beijnen, J. H., van der Houwen, O. A. G. J., and Underberg, W. J. M. (1986). Aspects of the degradation kinetics of doxorubicin in aqueous solution. *Int. J. Pharm.* 32 (2–3), 123–131. doi:10.1016/0378-5173(86)90170-5

Ceresa, C., Bravin, A., Cavaletti, G., Pellei, M., and Santini, C. (2014). The combined therapeutical effect of metal-based drugs and radiation therapy: the present status of research. *Curr. Med. Chem.* 21 (20), 2237–2265. doi:10.2174/09298673216614021612572l

Chang, D., Gao, Y., Wang, L., Liu, G., Chen, Y., Wang, T., et al. (2016). Polydopamine-based surface modification of mesoporous silica nanoparticles as pH-sensitive drug delivery vehicles for cancer therapy. *J. Colloid Interface Sci.* 463, 279–287. doi:10.1016/j.jcis.2015.11.001

Chang, Y. S., Adnane, J., Trail, P. A., Levy, J., Henderson, A., Xue, D., et al. (2007). Sorafenib (BAY 43-9006) inhibits tumor growth and vascularization and induces tumor apoptosis and hypoxia in RCC xenograft models. *Cancer Chemother. Pharmacol.* 59 (5), 561–574. doi:10.1007/s00280-006-0393-4

Chen, Y., Meng, Q., Wu, M., Wang, S., Xu, P., Chen, H., et al. (2014). Hollow mesoporous organosilica nanoparticles: a generic intelligent framework-hybridization approach for biomedicine. *J. Am. Chem. Soc.* 136 (46), 16326–16334. doi:10.1021/ja508721y

Dash, S., Murthy, P. N., Nath, L., and Chowdhury, P. (2010). Kinetic modeling on drug release from controlled drug delivery systems. *Acta pol. Pharm.* 67 (3), 217–223.

Dembereldorj, U., Kim, M., Kim, S., Ganbold, E. O., Lee, S. Y., and Joo, S. W. (2012). A spatiotemporal anticancer drug release platform of PEGylated graphene oxide triggered by glutathione *in vitro* and *in vivo*. *J. Mater. Chem.* 22 (45), 23845–23851. doi:10.1039/c2jm34853e

Du, J., Wang, L., Han, X., Dou, J., Jiang, X., and Yuan, J. (2021). Polydopamine/keratin complexes as gatekeepers of mesoporous silica nanoparticles for pH and GSH dual responsive drug delivery. *Mater. Lett.* 293, 129676. doi:10.1016/j.matlet.2021.129676

Folkman, J., and Long, D. M. (1964). The use of silicone rubber as a carrier for prolonged drug therapy. *J. Surg. Res.* 4 (3), 139–142. doi:10.1016/S0022-4804(64)80040-8

Gao, Y., Gao, D., Shen, J., and Wang, Q. (2020). A review of mesoporous silica nanoparticle delivery systems in chemo-based combination cancer therapies. *Front. Chem.* 8 (November), 598722–598817. doi:10.3389/fchem.2020.598722

Geng, H., Zhao, Y., Liu, J., Cui, Y., Wang, Y., Zhao, Q., et al. (2016). Hollow mesoporous silica as a high drug loading carrier for regulation insoluble drug release. *Int. J. Pharm.* 510 (1), 184–194. doi:10.1016/j.ijpharm.2016.05.067

Gisbert-Garzarán, M., and Vallet-Regí, M. (2021). Redox-responsive mesoporous silica nanoparticles for cancer treatment: recent updates. *Nanomaterials* 11 (9), 2222. doi:10.3390/nano11092222

Grześkowiak, B. F., Maziukiewicz, D., Kozłowska, A., Kertmen, A., Coy, E., and Mrówczyński, R. (2021). Polyamidoamine dendrimers decorated multifunctional polydopamine nanoparticles for targeted chemo-and photothermal therapy of liver cancer model. *Int. J. Mol. Sci.* 22 (2), 738–816. doi:10.3390/ijms22020738

Guan, Q., Guo, R., Huang, S., Zhang, F., Liu, J., Wang, Z., et al. (2020). Mesoporous polydopamine carrying sorafenib and SPIO nanoparticles for MRI-guided ferroptosis cancer therapy. *J. Control. Release* 320 (January), 392–403. doi:10.1016/j.jconrel.2020.01.048

Hao, Y. N., Zheng, A. Q., Guo, T. T., Shu, Y., Wang, J. H., Johnson, O., et al. (2019). Glutathione triggered degradation of polydopamine to facilitate controlled drug release for synergic combinational cancer treatment. *J. Mater. Chem. B* 7 (43), 6742–6750. doi:10.1039/c9tb01400d

Hermans, A., Abend, A. M., Kesisoglou, F., Flanagan, T., Cohen, M. J., Diaz, D. A., et al. (2017). Approaches for establishing clinically relevant dissolution specifications for immediate release solid oral dosage forms. *AAPS J.* 19 (6), 1537–1549. doi:10.1208/s12248-017-0117-1

Hu, L., Ma, J., Wei, X., Li, Y., Jiang, S., Ji, X., et al. (2022). Biodegradable polydopamine and tetrasulfide bond co-doped hollowed mesoporous silica nanospheres as GSH-triggered nanosystem for synergistic chemo-photothermal therapy of breast cancer. *Mater. and Des.* 215, 110467. doi:10.1016/J.MATDES.2022.110467

Kankala, R. K., Han, Y. H., Xia, H. Y., Wang, S. B., and Chen, A. Z. (2022). Nanoarchitectured prototypes of mesoporous silica nanoparticles for innovative biomedical applications. *J. Nanobiotechnology* 20 (1), 126–167. doi:10.1186/s12951-022-01315-x

Karwicka, E. (2010). Rola glutationu w oporności wielolekowej nowotworów. *Postępy Biol. Komórki* 2 (November), 323–341. Available at: http://www.hindawi.com/archive/2010/430939/.

Kim, H., Lee, D., Kim, J., Kim, T.Il, and Kim, W. J. (2013). Photothermally triggered cytosolic drug delivery via endosome disruption using a functionalized reduced graphene oxide. *ACS Nano* 7 (8), 6735–6746. doi:10.1021/nn403096s

Langer, R. (1998). Drug delivery and targeting. *Nature* 392 (6679 Suppl. l), 5–10. doi:10.1016/s0378-5173(02)00260-0

Li, Q. L., Xu, S. H., Zhou, H., Wang, X., Dong, B., Gao, H., et al. (2015). PH and glutathione dual-responsive dynamic cross-linked supramolecular network on mesoporous silica nanoparticles for controlled anticancer drug release. *ACS Appl. Mater. and Interfaces* 7 (51), 28656–28664. doi:10.1021/acsami.5b10534

Li, X., Xie, C., Xia, H., and Wang, Z. (2018). PH and ultrasound dual-responsive polydopamine-coated mesoporous silica nanoparticles for controlled drug delivery. *Langmuir* 34 (34), 9974–9981. doi:10.1021/acs.langmuir.8b01091

Li T, T., Shi, S., Goel, S., Shen, X., Xie, X., Chen, Z., et al. (2019). Recent advancements in mesoporous silica nanoparticles towards therapeutic applications for cancer. *Acta Biomater.* 89, 1–13. doi:10.1016/j.actbio.2019.02.031

Li X, X., Gao, F., Dong, Y., and Li, X. (2019). Strategies to regulate the degradability of mesoporous silica-based nanoparticles for biomedical applications. *Nano* 14 (12), 1930008–1930013. doi:10.1142/S1793292019300081

Luo, Z., Cai, K., Hu, Y., Zhao, L., Liu, P., Duan, L., et al. (2011). Mesoporous silica nanoparticles end-capped with collagen: redox-responsive nanoreservoirs for targeted drug delivery. *Angew. Chem.* 123 (3), 666–669. doi:10.1002/ange.201005061

Martínez-Carmona, M., Baeza, A., Rodriguez-Milla, M. A., García-Castro, J., and Vallet-Regí, M. (2015). Mesoporous silica nanoparticles grafted with a light-responsive protein shell for highly cytotoxic antitumoral therapy. *J. Mater. Chem. B* 3 (28), 5746–5752. doi:10.1039/c5tb00304k

Mokhtari, N., Taymouri, S., Mirian, M., and Dinari, M. (2020). Covalent triazine-based polyimine framework as a biocompatible pH-dependent sustained-release nanocarrier for sorafenib: an *in vitro* approach. *J. Mol. Liq.* 297, 111898. doi:10.1016/j.molliq.2019.111898

Mrówczyński, R. (2018). Polydopamine-based multifunctional (Nano)materials for cancer therapy. *ACS Appl. Mater. and Interfaces* 10 (9), 7541–7561. doi:10.1021/acsami.7b08392

Mrówczyński, R., Markiewicz, R., and Liebscher, J. (2016). Chemistry of polydopamine analogues. *Polym. Int.* 65 (11), 1288–1299. doi:10.1002/pi.5193

Mrówczyński, R., Nan, A., Turcu, R., Leistner, J., and Liebscher, J. (2015). Polydopamine - a versatile coating for surface-initiated ring-opening polymerization of lactide to polylactide. *Macromol. Chem. Phys.* 216 (2), 211–217. doi:10.1002/macp.201400380

Muhammad, F., Guo, M., Qi, W., Sun, F., Wang, A., Guo, Y., et al. (2011). PH-triggered controlled drug release from mesoporous silica nanoparticles via intracelluar dissolution of ZnO nanolids. *J. Am. Chem. Soc.* 133 (23), 8778–8781. doi:10.1021/ja200328s

Muhammad, F., Guo, M., Wang, A., Zhao, J., Qi, W., Guo, Y., et al. (2014). Responsive delivery of drug cocktail via mesoporous silica nanolamps. *J. Colloid Interface Sci.* 434, 1–8. doi:10.1016/j.jcis.2014.07.024

Noh, J., Kwon, B., Han, E., Park, M., Yang, W., Cho, W., et al. (2015). Amplification of oxidative stress by a dual stimuli-responsive hybrid drug enhances cancer cell death. *Nat. Commun.* 6, 6907. doi:10.1038/ncomms7907

Paarakh, M. P., Jose, P. A. N. I., Setty, C. M., and Peter, G. V. (2019). Release kinetics – concepts and applications. *Int. J. Pharm. Res. and Technol.* 8 (1), 12–20. doi:10.31838/ijprt/08.01.02

Panieri, E., and Santoro, M. M. (2016). Ros homeostasis and metabolism: a dangerous liaison in cancer cells. *Cell Death and Dis.* 7 (6), 22533–e2312. doi:10.1038/cddis.2016.105

Petros, R. A., and Desimone, J. M. (2010). Strategies in the design of nanoparticles for therapeutic applications. *Nat. Rev. Drug Discov.* 9 (8), 615–627. doi:10.1038/nrd2591

Porciani, D., Tedeschi, L., Marchetti, L., Citti, L., Piazza, V., Beltram, F., et al. (2015). Aptamer-mediated codelivery of doxorubicin and NF-κB decoy enhances chemosensitivity of pancreatic tumor cells. *Mol. Ther. - Nucleic Acids* 4 (4), e235. doi:10.1038/mtna.2015.9

Samaha, D., Shehayeb, R., and Kyriacos, S. (2009). Modeling and comparison of dissolution profiles of diltiazem modified-release formulations. *Dissolution Technol.* 16 (2), 41–46. doi:10.14227/DT160209P41

Shah, V. P., Tsong, Y., Sathe, P., and Liu, J. P. (1998). *In vitro* dissolution profile comparison- Statistics and analysis of the similarity factor, f2. *Pharm. Res.* 15 (6), 889–896. doi:10.1023/A:1011976615750

Shi, J., Votruba, A. R., Farokhzad, O. C., and Langer, R. (2010). Nanotechnology in drug delivery and tissue engineering: from discovery to applications. *Nano Lett.* 10 (9), 3223–3230. doi:10.1021/nl102184c

Singhvi, G., and Singh, M. (2011). International journal of pharmaceutical studies and research REVIEW: *IN-VITRO* DRUG RELEASE CHARACTERIZATION MODELS. *Int. J. Pharm. Stud. Res.* II (1), 77–84.

Swietach, P. (2019). What is pH regulation, and why do cancer cells need it? *Cancer Metastasis Rev.* 38 (1–2), 5–15. doi:10.1007/s10555-018-09778-x

Tang, H., Chen, D., Li, C., Zheng, C., Wu, X., Zhang, Y., et al. (2019). Dual GSH-exhausting sorafenib loaded manganese-silica nanodrugs for inducing the ferroptosis of hepatocellular carcinoma cells. In *International journal of pharmaceutics, international journal of pharmaceutics* 572. 118782, Elsevier B.V. doi:10.1016/j.ijpharm.2019.118782

Tao, W., Zhang, J., Zeng, X., Liu, D., Liu, G., Zhu, X., et al. (2015). Blended nanoparticle system based on miscible structurally similar polymers: a safe, simple, targeted, and surprisingly high efficiency vehicle for cancer therapy. *Adv. Healthc. Mater.* 4 (8), 1203–1214. doi:10.1002/adhm.201400751

Vallet-Regí, M., Colilla, M., Izquierdo-Barba, I., and Manzano, M. (2017). Mesoporous silica nanoparticles for drug delivery: current insights. *Molecules* 23 (1), 47–19. doi:10.3390/molecules23010047

Wang, K., Lu, J., Li, J., Gao, Y., Mao, Y., Zhao, Q., et al. (2021). Current trends in smart mesoporous silica-based nanovehicles for photoactivated cancer therapy. *J. Control. Release* 339 (July), 445–472. doi:10.1016/j.jconrel.2021.10.005

Wang, X., Zhang, J., Wang, Y., Wang, C., Xiao, J., Zhang, Q., et al. (2016). Multi-responsive photothermal-chemotherapy with drug-loaded melanin-like nanoparticles for synergetic tumor ablation. *Biomaterials* 81, 114–124. doi:10.1016/j.biomaterials.2015.11.037

Wei, Y., Gao, L., Wang, L., Shi, L., Wei, E., Zhou, B., et al. (2017). Polydopamine and peptide decorated doxorubicin-loaded mesoporous silica nanoparticles as a targeted drug delivery system for bladder cancer therapy. *Drug Deliv.* 24 (1), 681–691. doi:10.1080/10717544.2017.1309475

Wilhelm, S., Carter, C., Lynch, M., Lowinger, T., Dumas, J., Smith, R. A., et al. (2006). Discovery and development of sorafenib: a multikinase inhibitor for treating cancer. *Nat. Rev. Drug Discov.* 5 (10), 835–844. doi:10.1038/nrd2130

Woźniak, A., Walawender, M., Tempka, D., Coy, E., Załęski, K., Grześkowiak, B. F., et al. (2017). *In vitro* genotoxicity and cytotoxicity of polydopamine-coated magnetic nanostructures. *Toxicol. Vitro* 44, 256–265. doi:10.1016/j.tiv.2017.07.022

Xie, M., Shi, H., Ma, K., Shen, H., Li, B., Shen, S., et al. (2013). Hybrid nanoparticles for drug delivery and bioimaging: mesoporous silica nanoparticles functionalized with carboxyl groups and a near-infrared fluorescent dye. *J. Colloid Interface Sci.* 395 (1), 306–314. doi:10.1016/j.jcis.2013.01.001

Yang, P., Zhang, S., Chen, X., Liu, X., Wang, Z., and Li, Y. (2020). Recent developments in polydopamine fluorescent nanomaterials. *Mater. Horizons* 7 (3), 746–761. doi:10.1039/c9mh01197h

Zajda, J., Wróblewska, A., Ruzik, L., and Matczuk, M. (2021). Methodology for characterization of platinum-based drug's targeted delivery nanosystems. *J. Control. Release* 335 (March), 178–190. doi:10.1016/j.jconrel.2021.05.022

Zhang, Y., Huo, M., Zhou, J., Zou, A., Li, W., Yao, C., et al. (2010). DDSolver: an add-in program for modeling and comparison of drug dissolution profiles. *AAPS J.* 12 (3), 263–271. doi:10.1208/s12248-010-9185-1

Zheng, G., Zhao, R., Xu, A., Shen, Z., Chen, X., and Shao, J. (2018). Co-delivery of sorafenib and siVEGF based on mesoporous silica nanoparticles for ASGPR mediated targeted HCC therapy. *Eur. J. Pharm. Sci.* 111 (October 2017), 492–502. doi:10.1016/j.ejps.2017.10.036

Zheng, Q., Lin, T., Wu, H., Guo, L., Ye, P., Hao, Y., et al. (2014). Mussel-inspired polydopamine coated mesoporous silica nanoparticles as pH-sensitive nanocarriers for controlled release. *Int. J. Pharm.* 463 (1), 22–26. doi:10.1016/j.ijpharm.2013.12.045